ELECTROCHEMICAL STUDY OF GRAPHENE AND ITS OXIDIZED FORM

K. F. Chong[1]

[1]Faculty of Industrial Sciences and Technology, Universiti Malaysia Pahang,
Lebuhraya Tun Razak, 26300 Gambang, Kuantan, Pahang

Email: [1]ckfeng@ump.edu.my

ABSTRACT

Two types of graphene samples were electrochemically studied namely the as-synthesized graphene sample and the oxidized graphene sample. The electrochemical response was evaluated using Fe(CN)63-/4-, and Ru(NH3)62+/3+. The comparison was made based on the apparent heterogeneous electron transfer rate constant, and charge transfer resistance. Both graphene samples demonstrate extremely low background current which is the excellent criterion in designing biosensor. The introduction of higher carbon-oxygen functionalities on oxidized graphene exhibits lower electron transfer rate constant as compared to the as-synthesized graphene. Furthermore, oxidized graphene sample shows the excellent properties in resisting biofouling of β-nicotinamide adenine dinucleotide (NADH) and achieves detection limit of 10 nM. It shows that the oxygen functionalities on graphene surface renders it to be an excellent candidate for sensitive biosensor.

KEYWORDS: *graphene, electrochemical, biofouling, NADH.*

1.0 INTRODUCTION

Graphene consists of sp2-bonded carbon atoms arranged in a dense honeycomb crystal structure. It possesses semimetallic behavior with the small overlap between the valence and the conduction band or known as the zero-gap material (Lemme *et. al.*, 2007). The unique quantum properties of graphene such as quantum Hall effect, massless Dirac quasiparticles (Novoselov *et. al.*, 2005) and symmetries of wave functions, have attracted intense attention from both the experimental and theoretical scientific communities in recent years (Novoselov *et. al.*, 2004). The high carrier mobilities[3] of 15000 cm^{2+}/V, ballistic transport, and two dimensional (2D) nature of graphene make it a promising candidate for various applications in microelectronic devices, such as battery (Cassagneau *et. al.*, 1998), field effect transistor (Gilje *et. al.*, 2007), ultrasensitive sensors (Schedin *et. al.,* 2007) and electromechanical resonators (Bunch *et. al.,* 2007). We report herein an investigation of the electrochemical properties of graphene film synthesized by the thermal desorption of silicon on SiC. The as-synthesized graphene was further electrochemically oxidized in mild acidic condition in order to increase the carbon-oxygen functionalities on the graphene surface. Redox systems of $Fe(CN)_6^{3-/4}$ and $Ru(NH_3)_6^{2+/3+}$ were used to assess the electrochemical behavior of the as-synthesized graphene and graphene sample after oxidation. Finally, β-nicotinamide adenine dinucleotide (NADH) was selected as the biomolecules to evaluate the biosensing properties of graphene samples. The determination of NADH is vital because NADH and its oxidized form (NAD^+) are the coenxzymes for a large number of dehydrogenase enzymes and components of biomarker systems (Pariente *et. al.,* 1995; Wu *et. al.,* 1996; Pariente *et. al.,* 1997). However, the oxidation of NADH usually encounters low sensitivity problem due to its high overpotential (~0.8V) and biofouling of the electrode surface (Moiroux *et. al.,* 1978; Jacgfeldt *et. al.,* 1980; Bladael *et. al.,* 1975).

2.0 EXPERIMENTAL SECTION

2.1 Chemicals

All the chemicals used in this experiment were purchased from Sigma Aldrich unless otherwise stated and were used as received. The NADH solution was prepared and used freshly. All the solutions in this work were prepared in deionized water.

2.2 Graphene Preparation

Epitaxial graphene was fabricated on the silicon terminated (0001) face of high purity 6H-SiC by thermal desorption of silicon at high temperature (Zhou *et. al.,* 2007).

2.3 Electrode Preparation and Pretreatment

Electrical connection was done to the graphene by contacting copper wire to the graphene surface and mounting with silver paste. The electrical connection, backside and edge of the graphene sample were insulated with nail varnish. The as-synthesized graphene underwent mild oxidation by electrochemical oxidation at 2 V in 0.5 M H_2SO_4 for 60 seconds.

Hereafter, we denote the as-synthesized graphene as graphene sample and the graphene sample after mild oxidation as oxidized graphene.

2.4 Electrochemical Measurement

All electrochemical experiments in this work were accomplished by Autolab/PGSTAT30, Eco Chemie B.V. with platinum wire and saturated Ag/AgCl electrode as counter and reference electrode respectively. Cyclic voltammetry was performed at room temperature with different scan rates (step potential of 5 mV) and the measurement was repeated 3 times to obtain the reproducible signals. In every case, the last cycle was recorded. The amperometric measurement of NADH was done by collecting current response with time at constant potential of 0.75 V. A magnetic stirrer (100 rpm) was used to provide convective transport during the amperometric measurement. Electrochemical impedance spectroscopy (EIS) was carried out with Autolab Frequency Response Analyzer (FRA). The impedance data was collected from 500kHz to 0.01 Hz, at an ac amplitude of 10 mV and performed at open circuit potential (OCP). 1 M KCl was used as the working electrolyte for redox species throughout the electrochemical measurements and 0.1 M phosphate buffer solution was used as the working electrolyte for NADH measurement.

3.0 RESULTS AND DISCUSSIONS

Figure 1 shows the representative background cyclic voltammograms for graphene and oxidized graphene electrodes in blank electrolyte 1 M KCl at 100 mV s^{-1}. To make a clear comparison, the reported currents have been normalized to the exposed surface area. The background cyclic voltammetry is very useful to evaluate the graphene electrode surface as the electrochemical response is highly sensitive to the physicochemical properties of the electrode. Graphene electrode possesses working potential window of 1.7 V with low and featureless background current in the region between -0.35 V and 1.35 V. There is no evidence for any surface redox process occurs on graphene surface between -0.35 V to 0.9 V, indicating that graphene is ideally polarizable in this potential region. On the other hand, oxidized graphene is observed to have narrower working potential window, i.e. 1.35 V, though it also exhibits low background current. Both graphene samples show anodic peak on the forward sweep at 1.1 V, which can be attributed to the oxidation of sp^2 carbon and electrochemically-active carbon-oxygen functionalities. It can be seen that oxidized graphene shows higher anodic current at 1.1 V because the oxidation of graphene surface has increased the carbon-oxygen functionalities on the surface. Both graphene samples also show the similarity in the onset potential for hydrogen evolution but the oxidized graphene exhibits lower onset potential for chlorine evolution. As comparison, wide electrochemical window material, i.e. boron-doped diamond electrode has been inserted into the graph for comparison. In order to have a clear view of the capacitive background current, three voltammograms (boron-doped diamond, graphene and oxidized graphene voltammograms) are stacked together as displayed in Figure 2. Interestingly, both graphene samples exhibits low background current as compared to boron-doped diamond. At 0 V, capacitive background current for graphene (0.85 μA cm^{-2}) is about 3.5 times lower than the boron-doped diamond (3.08 μA cm^{-2}) while capacitive background current for oxidized graphene (1.46 μA cm^{-2}) is about 2 times lower than the boron-doped diamond. The increment of capacitive background current for oxidized graphene as compared to graphene can be attributed to the increase of carbon-oxygen functionalities on the surface which will lead to charging of the surface. Both graphene samples show stable surface microstructure as no change can be observed after multiple cycle scans.

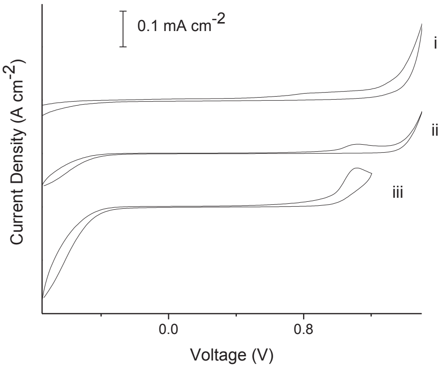

Figure 1 Electrochemical window of (i) boron-doped diamond, (ii) graphene, (iii) oxidized graphene in 1 M KCl.

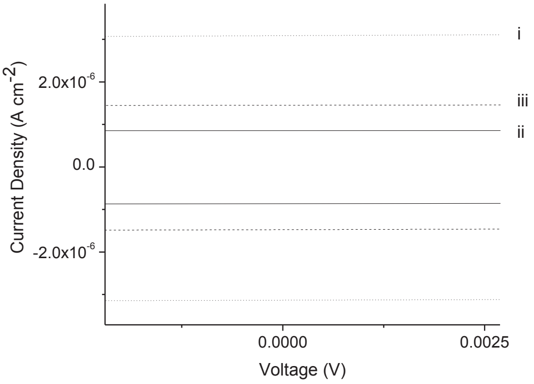

Figure 2 Background current of (i) boron-doped diamond, (ii) graphene, (iii) oxidized graphene in 1 M KCl.

Redox systems of $Fe(CN)_6^{3-/4-}$ and $Ru(NH_3)_6^{2+/3+}$ were chosen to evaluate the sensitivity of each redox system to the surface microstructure and electronic properties of graphene samples. The apparent electron transfer rate constants $k°_{app}$ (calculated with Nicholson's method) for the redox systems are summarized in Table 1. Peak currents for the redox systems vary linearly with square root scan rate for both graphene and oxidized graphene samples, an indication of the semi-infinite linear diffusion of the redox species on the samples surface.

$Fe(CN)_6^{3-/4-}$ is chosen as redox probe because the electrode reaction kinetics for this redox couple are strongly influenced by the fraction of exposed edge plane on *sp*^{2}-bonded carbon electrode and the surface cleanliness (Chen et al., 1996). Figure 3 shows that $Fe(CN)_6^{3-/4-}$ redox reaction is near-Nernstian (ΔE_p = 73 mV) on graphene surface. After undergo mild oxidation on graphene surface, the current response for oxidized graphene is reduced, accompanied by the increase in ΔE_p. Furthermore, graphene shows 2 times higher in $k°_{app}$ for $Fe(CN)_6^{3-/4-}$ redox system as compared to the oxidized graphene. It is found that the higher surface termination of oxygen on oxidized graphene will lower down the electron transfer of $Fe(CN)_6^{3-/4-}$. However, this redox reaction is still reversible on oxidized graphene. This can be explained by the fact that the oxidized graphene only undergoes very mild electrochemical oxidation; hence the complete coverage of oxygen functionalities on the surface is not achieved.

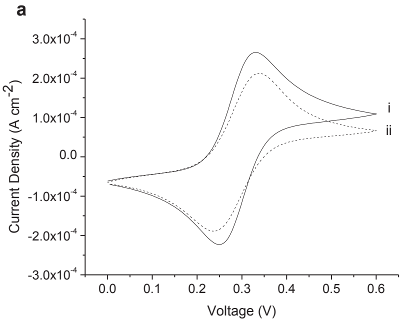

Figure 3 Cyclic voltammograms of (i) graphene, (ii) oxidized graphene in 1 mM $Fe(CN)_4^{3-/4-}$.

$Ru(NH_3)_6^{2+/3+}$ is chosen as the redox probe as it only involves simple electron transfer on the electrode and the reaction rate is largely affected by the electronic properties of the electrode. The electrode kinetics for $Ru(NH_3)_6^{2+/3+}$ are relatively insensitive to the surface microstructure, surface functionalities or adsorbed layers. Figure 4 shows that $Ru(NH_3)_6^{2+/3+}$ exhibits near-Nernstian redox reaction on both graphene and oxidized graphene with the same current response, same ΔE_p and same k°_{app}. This is an indication that the mild electrochemical oxidation does not change the electronic properties of graphene and it merely increases the oxygen functionalities on the surface.

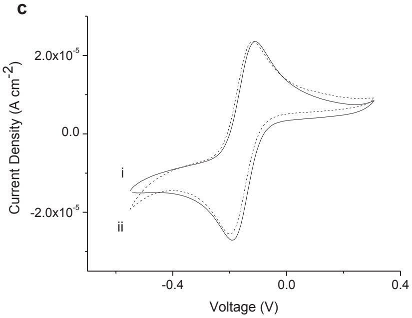

Figure 4 Cyclic voltammograms of (i) graphene, (ii) oxidized graphene in 1 mM $Ru(NH_3)_6^{2+/3+}$.

Table 1 Comparison of apparent electon transfer rate constant, $k°_{app}$

Redox species	**$k°_{app}$ (cm s^{-1})**	
	Graphene	**Oxidized Graphene**
$Fe(CN)_6^{3-/4-}$	5.02×10^{-3}	2.51×10^{-3}
$Ru(NH_3)_6^{2+/3+}$	3.27×10^{-3}	2.91×10^{-3}

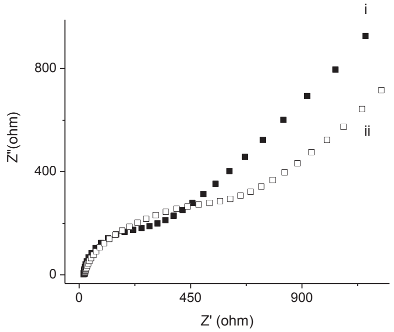

Figure 5 Nyquist plot of (i)graphene, (ii) oxidized graphene in 1 mM $Fe(CN)_6^{3-/4-}$.

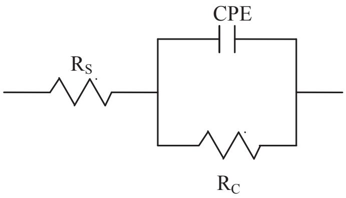

Schematic 1 Randles equivalent circuit model for graphene and oxidized graphene in 1 mM $Fe(CN)_6^{3-/4-}$.

Figure 5 shows that Nyquist plot of both grahene and oxidized graphene samples show similar behavior at open circuit potential (OCP): a small semicircle follower by a 45° straight line. This implies that the charge transfer resistance (R_{CT}) across both graphene samples is small and limited only by Warburg diffusion. The impedance data of both graphene samples are fitted into simple Randles equivalent circuit model as depicted in Schematic 1 and the R_{CT} values are extracted from the model. Under similar experimental condition, the R_{CT} for oxidized graphene is almost 2 orders of magnitude higher than the R_{CT} for graphene. It implies that the mild oxidation process on graphene surface will impart a charge transfer barrier for $Fe(CN)_6^{3-/4-}$ electrolyte, consistent with the higher $k°_{app}$ finding on oxidized graphene.

In order to develop the graphene material into electrochemical biosensor for continuous monitoring of biomolecules, electrochemical stability of the electrode towards biomolecules is very crucial. In this work, NADH is selected as the biomolecules for electrochemical stability testing. However, direct oxidation of NADH at bare electrode occurs at high overpotential (~0.8 V) and is usually accompanied by the electrode fouling problem by its oxidation product (NAD+). The electrochemical oxidation of NADH on bare glassy carbon electrodes was anodically shifted and deactivated rapidly due to the irreversibly adsorption of NAD+ (Moiroux *et. al.*, 1978). In order to reduce the fouling problem and the overpotential problem, electrochemical pretreatment on glassy carbon electrode was applied (Engstrom *et. al.*, 1984; Hayes *et. al.*, 1999). However, such pretreatment was overwhelmed by the increase in detection limit due to the increase in background current after pretreatment. The carbon nanotube modified electrode was found to possess anti-fouling and lower detection potential towards NADH oxidation (Musameh *et. al.*, 2002; Valentini *et. al.*, 2003). However, it is difficult to obtain low detection limit using this carbon nanotube modified electrode because of its high background current due to its large surface roughness.

Figure 6 and Figure 7 show the cyclic voltammograms for 5 μM NADH on graphene and oxidized graphene. The solid lines in the cyclic voltammograms represent the 1st cycle while the dotted lines represent the 20th cycle. On the 1st scan, both graphene and oxidized graphene electrodes exhibit a clear NADH oxidation peak at 0.64 V. However, there is difference between both electrodes after continuous scan for 20 cycles. We can observe a drastic drop in NADH oxidation peak current for graphene electrode, an indication for the surface fouling caused by the adsorption of NAD+. In contrast, we are able to obtain stable oxidation peak currents for oxidized graphene electrode under the same measurement conditions and the peak currents remain unchanged after 20 scan cycles. Hence, we conclude that the mild electrochemical oxidation on graphene surface will increase its resistance towards NAD+ surface fouling.

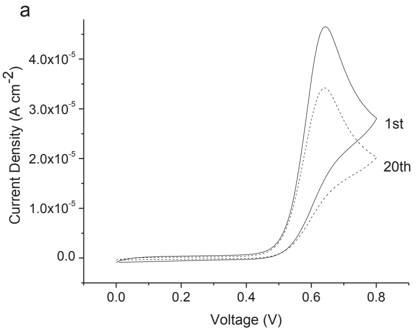

Figure 6 Cyclic voltammograms for 5 μM NADH in 0.1 M PBS at graphene electrode at 100 mV s^{-1}.

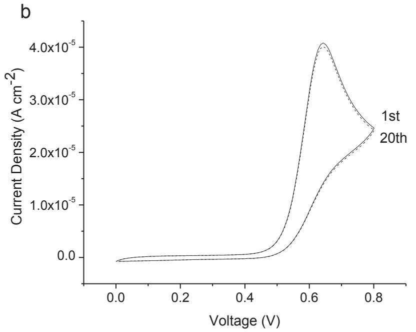

Figure 7 Cyclic voltammograms for 5 μM NADH in 0.1 M PBS at oxidized graphene electrode at 100 mV s^{-1}.

With extremely low background current and surface fouling resistance on oxidized graphene surface, it is further tested on NADH on the detection limit aspect. The detection limit is tested with amperometry experiment with constant voltage of 0.75 V. Figure 8 summarizes the calibration curve for NADH oxidation on oxidized graphene electrode. The current response is increased with increasing NADH concentration and the linearity range is from 10 nM to 5 μM. The detection limit of oxidized graphene for NADH is found to be 10 nM (S/N=3) as shown in Figure 9. This result indicates that the graphene after mild electrochemical oxidation is a useful electrode material for analytical detection of NADH, making it an attractive platform for the enzyme-catalyzed biosensor, which involves NADH as cofactor.

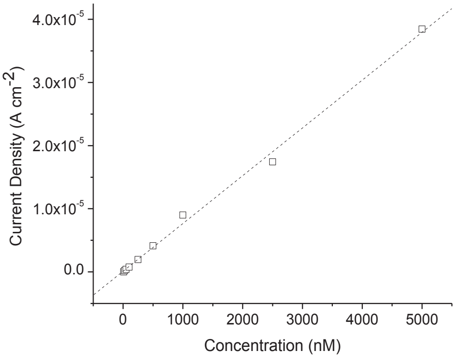

Figure 8 Calibration curve of NADH oxidation current at oxidized graphene electrode.

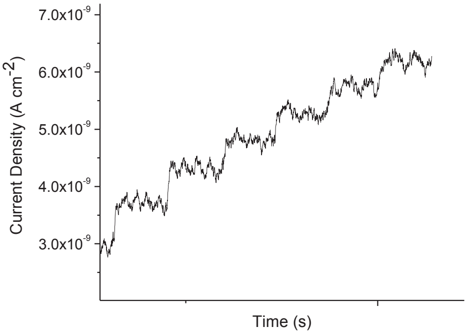

Figure 9 Amperometry of oxidized graphene electrode towards addition of 10 nM NADH.

4.0 CONCLUSION

The electrochemical properties of graphene materials are investigated before and after mild electrochemical oxidation. Both graphene materials show extremely low background current and it is slightly increased after oxidation process. Nevertheless, this low background current behavior for graphene material renders it a superb material in analytical measurement. The electrochemical activities of graphene are tested in different redox systems. It is found that graphene material possesses higher charge transfer resistance after mild electrochemical oxidation. Though the oxidation process on graphene material will lower down its electrochemical activities towards certain redox systems, it shows excellent properties in resisting biofouling problem created by the oxidation of NADH and a low detection limit (10 nM) for NADH can be achieved.

5.0 ACKNOWLEDGEMENT

The project is funded under UMP RDU100352 and the author would like to thank National University of Singapore for the facilities support.

6.0 REFERENCES

M. C. Lemme, T. J. Echtermeyer,M. Baus, H. Kurz. 2007. Vol. 28. 282.

K. S. Novoselv, A. K. Geim, S. V. Morozov, D. Jiang, M. I. Katsnelson, I. V. Grigorieva, S. V. Dubonos, A. A. Firsov. 2005. Nature. Vol. 438. 197.

K. S. Novoselv, A. K. Geim, S. V. Morozov, D. Jiang, Y. Zhang, S. V. Dubonos, I. V. Grigorieva, A. A. Firsov. 2004. Science. Vol. 306. 666.

T. Cassagneau, J. H. Fendler. 1998. Adv. Mater. Vol. 10. 877.

S. Gilje, S. Han, M. Wang, K. L. Wang, R. B. Kaner. 2007. Nano Lett. Vol. 7. 3394.

F. Schedin, A. K. Geim, S. V. Morozov, E. W. Hill, P. Blake, M. I. Katsnelson, K. S. Novoselov. 2007. Nat. Mater. Vol. 6. 652.

J. S. Bunch, A. M. van der Zande, S. S. Verbridge, I. W. Frank, D. M. Tanenbaum, J. M. Parpia, H. G. Craighead, P. L. McEuen. 2007. Science. Vol. 315. 490.

F. Pariente, E. Lorenzo, F. Tobalina, H. D. Abruna.1995. Anal. Chem. Vol. 67. 3936.

Q. Wu, M. Maskus, F. Pariente, F. Tobalina, V. M. Fernández, E. Lorenzo, H. D. Abruna.1996. Anal. Chem. Vol. 68. 3688.

F. Pariente, F. Tobalina, G. Moreno, L. Hernandez, E. Lorenzo, H. D. Abruna. 1997. Anal. Chem. Vol. 69. 4065.

J. Moiroux, J. Elving. 1978. Anal. Chem. Vol. 50. 1056.

H. Jacgfeldt. 1980. J. Electroanal. Chem. Vol. 110. 295.

W. Blaedel, R, Jenkins. 1975. Anal. Chem. Vol. 47. 1337.

S. Y. Zhou, G. –H. Gweon, A. V. Fedorov, P. N. First, W. A. de Heer, D. –H. Lee, F. Guinea, A. H. Castro Neto, A. Lanzara. 2007. Nat. Mater. Vol. 6. 770.

P. Chen, R. L. McCreery. 1996. Anal. Chem. Vol. 68. 3958.

J. Moiroux, J. Elving. 1978. Anal. Chem. Vol. 8. 1056.

R. C. Engstrom, V. A. Strasser. 1984. Anal. Chem. Vol. 56. 136.

M. A. Hayes, W. G. Kuhr. 1999. Anal. Chem. Vol. 71. 1720.

M. Musameh, J. Wang, A. Merkoci, Y. Lin. 2002. Electrochem. Commun. Vol. 4. 743.

F. Valentini, A. Amine, S. Orlanducci, M. L. Terranova, G. Palleschi. 2003. Anal. Chem. Vol. 75. 5413.